



Research papers

Discrimination between the influences of river discharge and coastal upwelling on summer microphytoplankton phosphorus stress in the East China Sea



Hung-Chun Liu^a, Chi-Yu Shih^a, Gwo-Ching Gong^{b,c,d}, Tung-Yuan Ho^e, Fuh-Kwo Shiah^e, Chih-hao Hsieh^f, Jeng Chang^{a,b,c,*}

^a Institute of Marine Biology, National Taiwan Ocean University, Keelung 20224, Taiwan, ROC

^b Institute of Marine Environmental Chemistry and Ecology, National Taiwan Ocean University, Keelung 20224, Taiwan, ROC

^c Center of Excellence for the Oceans, National Taiwan Ocean University, Keelung 20224, Taiwan, ROC

^d Taiwan Ocean Research Institute, National Applied Research Laboratories, Jiading, Kaoshiung 852, Taiwan, ROC

^e Research Center for Environmental Changes, Academia Sinica, Nankang, Taipei 115, Taiwan, ROC

^f Institute of Oceanography and Institute of Ecology and Evolutionary Biology, National Taiwan University, Taipei 10617, Taiwan, ROC

ARTICLE INFO

Article history:

Received 15 November 2012

Received in revised form

19 March 2013

Accepted 3 April 2013

Available online 15 April 2013

Keywords:

Alkaline phosphatase activity

Phosphate stress

Microphytoplankton

Changjiang discharge

Coastal upwelling

East China Sea

ABSTRACT

The status of summer microphytoplankton phosphorus stress in the East China Sea (ECS) was evaluated by alkaline phosphatase activity (APA) and the maximum quantum efficiency of photosynthesis (F_v/F_m). During the study period in 2005–2008, values of APA ranged 0.19–1414 pmol PO_4^{3-} ($\mu\text{g Chl. a}^{-1} \text{min}^{-1}$) and those of F_v/F_m ranged 0.22–0.57. In general, low APA and high F_v/F_m occurred in the coastal zone as well as in the Changjiang (Yangtze River) plume, and high APA occurred in the mid-shelf region of the northern ECS. Based on regression analyses of APA and F_v/F_m , 2 mixing series that influenced the microphytoplankton phosphorus status were identified. Changjiang discharge with high nutrient concentrations and a high dissolved N:P ratio marked the starting point of the plume-driven mixing series. Along this mixing series, the river discharge gradually mixed with offshore waters, and microphytoplankton produced high APA values when the phosphate concentration dropped below $0.2 \mu\text{mol P L}^{-1}$. Coastal upwelling was observed to initiate a unique upwelling-driven mixing series in summer. As upwelled water mixed across the continental shelf, the utilization of nutrients caused low F_v/F_m values without a corresponding increase in the APA. The area of microphytoplankton showing symptoms of phosphorus stress in summer varied from year to year, and was closely related to the size of Changjiang plume and the strength of coastal upwelling.

© 2013 Elsevier Ltd. All rights reserved.

1. Introduction

River discharges are major nutrient sources that support primary production in coastal ecosystems. Due to the growth of agricultural and industrial activities for many decades, terrestrial export of nitrogen has significantly increased (Seitzinger et al., 2002). Although this increase in fixed nitrogen will eventually be balanced by accelerated denitrification rates (Canfield et al., 2010), the disproportionately enriched N and P are still observed in some coastal ecosystems, and cause decreases in primary production, changes in phytoplankton composition, and altered food web structures (Glibert, 2010). A precise identification of nitrogen- vs. phosphorus-controlled regions of coastal seas is thus crucial to

ecological modeling and the sustainable management of these ecosystems.

The East China Sea (ECS) is the largest marginal sea in the western North Pacific and is very productive. It is also a CO_2 sink with an annual uptake rate of $0.013\text{--}0.030 \text{ Gt C yr}^{-1}$ (Wang et al., 2000). The Changjiang (Yangtze River) is the major freshwater source that influences salinity and nutrient distributions in the ECS (Harrison et al., 1990; Gong et al., 1996). According to recent investigations (Gong et al., 1996; Wong et al., 1998), nitrogen concentrations are anomalously high in the area influenced by the Changjiang discharge, which implies that local phytoplankton may experience phosphorus stress. In addition, Harrison et al. (1990) pointed out that many large rivers in China have high nutrient loading with nitrogen in great excess of phosphorus, and bioassay experiments indicated that phytoplankton growth is P-limited in Xiamen Bay, a water body close to the southern border of the ECS. In summer, an additional nutrient source for the ECS is coastal upwelling driven by prevailing wind and currents (Chen et al.,

* Corresponding author at: Institute of Marine Biology, National Taiwan Ocean University, Keelung 20224, Taiwan, ROC. Tel.: +886 2 24622192x5308; fax: +886 2 24633152.

E-mail address: jengchang@mail.ntou.edu.tw (J. Chang).

2004). Nutrients brought by upwelling events usually have dissolved N:P ratios of < 16 , implying that nitrogen is more likely to become the controlling nutrient in upwelling-dominated regions.

Microphytoplankton, phytoplankton in the size range of 20–200 μm , are an important food source for copepods, and this trophic link contributes significantly to fish production (Sommer et al., 2002; Berglund et al., 2007). Due to their large size and high sinking rate, microphytoplankton are also a major contributor to sedimentation of organic particles (Falkowski, 2002; Kjørboe, 1993). In the ECS, microphytoplankton constitute a substantial portion in total phytoplankton. According to a recent survey (Chen, 2000), $26 \pm 18\%$ (mean \pm S.D.) of integrated Chl. *a* on the shelf proper came from organisms with a body size $> 20 \mu\text{m}$, but this percentage decreased to $10 \pm 4.1\%$ in the Kuroshio Current near the shelf break. In a coastal bloom, a chain-forming diatom, *Skeletonema costatum*, was the dominant microphytoplankton that contributed 75% of the total phytoplankton carbon (Chang et al., 2003). However, microphytoplankton's large size makes them more vulnerable to nutrient stress in marine ecosystems (Kjørboe, 1993). Thus their physiological status may significantly differ from the rest of phytoplankton community. In the ECS, Chen (2000) demonstrated that both the biomass and productivity of microplankton are more variable than those of picoplankton, which implies that microplankton more often experience growth limitations. As a result, nutrient concentration and stoichiometry heavily influence the dominant species in phytoplankton, and such influences will propagate along the food chain to shape the structure of entire pelagic community (Glibert, 2010; Sommer et al., 2002).

To confirm the existence of nutrient stress, ambient concentrations and molar ratios of chemical species are frequently used as criteria. However, to determine nutrient-stresses specific to microphytoplankton, methods that can measure stress-related activities in different size-classes are more suitable. All phytoplankton produce an extracellular enzyme, alkaline phosphatase (AP), to utilize organic phosphorus when ambient inorganic phosphate is exhausted (Perry, 1972; Dyrhman and Ruttenberg, 2006). This property leads to the use of AP activity (APA) as an indicator of phosphorus stress in both marine and freshwater environments, including several studies conducted in the ECS (Ou et al., 2006; Huang et al., 2007). Another nutrient-related physiological indicator in phytoplankton is the maximum quantum efficiency of photosynthesis (F_v/F_m). Nutrient deficiencies in phytoplankton due to phosphate, nitrate, and iron cause low F_v/F_m values by reducing electron transport in the light reaction (Geider et al., 1993; Wykoff et al., 1998). In oceanic and estuarine environments, low values of F_v/F_m were correlated with low concentrations of various nutrients (Kolber and Falkowski, 1993; Kromkamp and Peene, 1999), indicating close interactions between nutrient stress and photosynthesis. Some uncertainties may come from a cyanobacterium-dominated phytoplankton community. These organisms are known to have lower F_v/F_m values due to their phycobiliprotein-containing photosynthetic system (Campbell et al., 1998). In a study conducted in the southern ECS, F_v/F_m always decreased from the upwelling center toward the oligotrophic Kuroshio Current in June, August, and September, but a significant correlation between APA and F_v/F_m only occurred in September, suggesting the existence of phosphate stress in that month (Liu et al., 2010).

In this study, we conducted experiments to detect the presence of phosphorus stress in microphytoplankton during 4 cruises to the ECS in summer 2005–2008. The APA was used to assess the in situ P status of microphytoplankton. In addition, F_v/F_m was used to provide an independent evaluation of phytoplankton's physiological state. Our results indicated a clear zonation of phosphorus stress in the

ECS, which can be correlated to different nutrient sources and hydrographic conditions.

2. Materials and methods

2.1. Study sites, sampling, and Chl. *a* concentrations

Four oceanographic cruises to the ECS were conducted on board the R/V Ocean Researcher I or Ocean Researcher II (2006 only) during 9–17 June 2005, 23 June–4 July 2006, 1–11 July 2007, and 3–13 July 2008 (Fig. 1 and Table 1). In total, 28–34 stations were visited during individual cruises, and APA measurements were performed at 17–34 stations. The hydrographic parameters of temperature and salinity data were measured with a CTD (SBE 911 plus SeaBird, Bellevue, WA, USA). Samples for nutrient concentrations were collected by X-Niskin bottles at the same depth as microplankton samples (General Oceanics, Miami, FL, USA) mounted on a rosette sampler.

Microplankton samples for APA and F_v/F_m measurements were collected by a plankton net with a 0.5-m mouth diameter and 20- μm mesh size. The net was towed at depths of 5 m (2005 and 2007 cruises), 10 m (2006 cruise), and 1 m (2008 cruise) for 10 min with the ship speed set to 1 knot. According to our previous experiences, the volume of water filtered during a typical net-tow ranged 5800–48,000 L (Chang, 2000). Next, the content in the receiving bottle (cod end) was sequentially filtered through 1-mm, 200- μm , and 20- μm mesh Nitex screens. Phytoplankton retained on the 20- μm Nitex screen were washed down and resuspended in 300–1000 mL of seawater collected from the same depth.

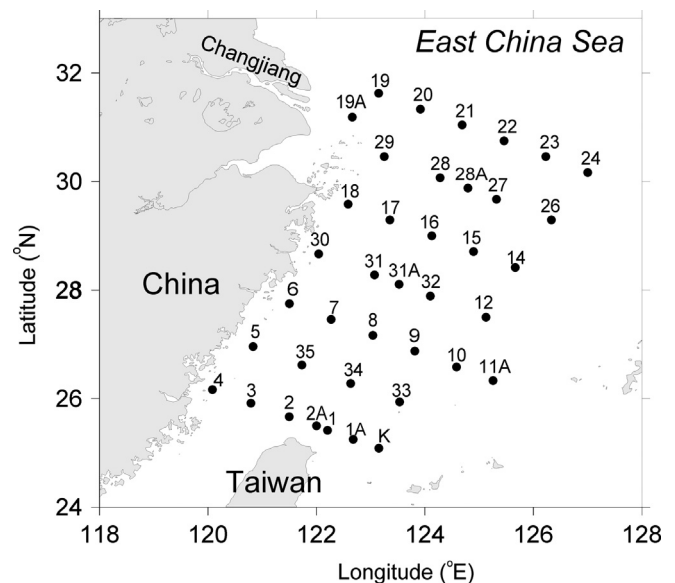


Fig. 1. Map of the East China Sea showing station locations during cruises conducted in June 2005, June–July 2006, July 2007, and July 2008.

Table 1

Oceanographic cruises to the East China Sea during the study period.

Date	Cruise number	Stations visited	APA ^c stations
9–17 June 2005	ORI ^a 756A	28	25
23 June–4 July 2006	ORII ^b 1360	33	17
1–11 July 2007	ORI 836	32	23
3–13 July 2008	ORI 870	34	34

^a R/V Ocean Researcher I.

^b R/V Ocean Researcher II.

^c Number of stations at which alkaline phosphatase activity was measured.

Triplicate subsamples of 4 mL were used for the APA measurement. In addition, a separate set of triplicate subsamples of 2 mL in volume was used for the F_v/F_m measurement (2007 and 2008 cruises only). Another subsample with a volume of 1–20 mL, depending on the concentration of phytoplankton, was filtered onto a GF/F filter (Whatman, Piscataway, NJ, USA) for chlorophyll *a* measurements. The GF/F filter was immediately packed into an aluminum foil (2005 and 2006 cruises) or a tissue-processing capsule (2007 and 2008 cruises, Electron Microscopy Sciences, Hatfield, UK), and stored in liquid nitrogen until analysis. The amount of Chl. *a* on the filters was determined fluorometrically by the Welschmeyer (1994) non-acidification method.

2.2. Alkaline phosphatase activity (APA)

To determine APA, 0.5 mL of the AP substrate, 3-O-methylfluorescein phosphate (Sigma, St. Louis, MO, USA), was added to a 4-mL subsample at a final concentration of $0.11 \mu\text{mol L}^{-1}$. Afterward, the subsample was incubated in the dark at 25°C for 60 min. At the beginning and end of the incubation period, fluorescence in the reaction mixture was measured with a fluorometer (10-AU, Turner Designs, Sunnyvale, CA, USA) equipped with a 390–500-nm band-pass excitation filter and a 510–700-nm band-pass emission filter (Perry, 1972). A standard curve was used to convert the fluorescence intensity to moles PO_4^{3-} released, and the releasing rate of PO_4^{3-} was normalized to the Chl-*a* in net-collected microplankton samples (Perry, 1972; Liu et al., 2010). Such obtained enzyme activity (APA) was expressed as $\text{pmol PO}_4^{3-} (\mu\text{g Chl. } a)^{-1} \text{ min}^{-1}$. For the measurement of P-suppressed APA, extra orthophosphate was added to a 4-mL subsample (final conc.: $36.3 \mu\text{mol P L}^{-1}$) followed by an incubation in darkness for 1 h. Next, APA substrate was added, and P-suppressed APA was determined as in a regular sample.

2.3. F_v/F_m measurements

To determine F_v/F_m , microphytoplankton subsamples with a volume of 2 mL were placed in quartz cuvettes (NSG Precision Cells, New York, NY, USA) and dark-adapted for 15 min (Campbell et al., 1998). The cuvettes were then placed in a Fluorescence Induction and Relaxation (FIRe) fluorometer (Satlantic, Halifax, NS, Canada), and a single turnover flash (at a wavelength of $450 \pm 15 \text{ nm}$) with a duration of 80 μs was applied to saturate PS II in phytoplankton cells. The minimum and maximum yields of Chl. *a* fluorescence (F_0 and F_m) were recorded at the beginning and end of the single turnover flash, and the maximum quantum efficiency of photosynthesis (F_v/F_m) was computed as $(F_m - F_0)/F_m$ (Campbell et al., 1998; Liu et al., 2010). The net-collected samples are high in chlorophyll content. Our preliminary test indicated that F_v/F_m values in the ECS microplankton samples did not change when either filtered seawater or distilled water was used as the blank (Cullen and Davis, 2003).

2.4. Determination of nutrient concentrations

The concentration of soluble reactive phosphate in the nutrient samples was measured by a modified version of the molybdenum blue method with a detection limit of $0.01 \mu\text{mol P L}^{-1}$ (Liu et al., 2010). In addition, nutrient samples at 5-m depth in July 2007 were first concentrated by the magnesium-induced coprecipitation (MAGIC) method before the use of molybdenum blue detection (Karl and Tien, 1997). The MAGIC method lowered the detection limit to 4 nmol P L^{-1} .

Nitrate in the seawater was first reduced to nitrite with a cadmium wire activated with copper sulfate, and the nitrite concentration was then measured by the pink azo dye method.

The measuring procedure was automated using a self-designed flow injection analyzer (Pai et al., 1990a, 1990b; Gong, 1992; Gong et al., 2000), and the detection limits of nitrate and nitrite were 0.3 and $0.03 \mu\text{mol N L}^{-1}$, respectively. The excess nitrate was computed according to the following equation (Wong et al., 1998):

$$N_{\text{ex}} = ([\text{NO}_3^-]) + ([\text{NO}_2^-]) - R[\text{DIP}] \quad (1)$$

where $[\text{NO}_3^-]$ and $[\text{NO}_2^-]$ are the concentrations of nitrate and nitrite, [DIP] is the concentration of dissolved inorganic phosphate, and R is the ratio of the biological utilization of [nitrate+nitrite] relative to phosphate by marine phytoplankton. The value of R used for ECS in Wong et al. (1998) was 14.5, and the same value was used in this study to make the results comparable.

2.5. Phytoplankton enumeration

Microphytoplankton cells were preserved with acidic Lugol's solution, and counted with a Nikon Optiphot-2 microscope (Nikon, Tokyo, Japan) at $100\times$ (Smayda, 1974). At least 100 cells were examined in each sample, and cells were identified to the generic level based on Tomas et al. (1996). The abundances of *Trichodesmium* spp. were counted in trichomes. An average length of 12.45 cells trichome $^{-1}$ ($n=100$) was used as the conversion factor based on a previous investigation in a segment of the Kuroshio Current near Taiwan.

2.6. Statistical data analysis

The method of quantile regression was employed to identify the position of median (0.5 quantile) APA at a given F_v/F_m , and a regression equation was generated to describe how median APA changed with F_v/F_m (Koenker and Hallock, 2001). The actual computation was performed using the “quantreg” package provided by the R project for statistical computing (<http://www.r-project.org/>). Next, relationships between APA and F_v/F_m for data points above and below the median APA equation were separately analyzed by regular linear regression.

3. Results

3.1. Range of variation in APA 2005–2008

During the study period in 2005–2008, ECS APA values in summer ranged $0.19\text{--}1414 \text{ pmol PO}_4^{3-} (\mu\text{g Chl. } a)^{-1} \text{ min}^{-1}$. The measured APA showed a left-skewed distribution with 85% of the values within $0\text{--}40 \text{ pmol PO}_4^{3-} (\mu\text{g Chl. } a)^{-1} \text{ min}^{-1}$. The overall mean and median were 39.5 and $13.8 \text{ pmol PO}_4^{3-} (\mu\text{g Chl. } a)^{-1} \text{ min}^{-1}$, respectively (Fig. 2A). In this study, APA values lower than the median were generally observed in the coastal zone and Changjiang plume, while high values were mainly observed in the mid-shelf region (Fig. 3M–P).

3.2. Distributions of Changjiang plume, DIP, N_{ex} , and APA in 2005

The Changjiang plume was distributed in a narrow zone along the coast in June 2005 when the 31 isohaline was used as the outer limit (Fig. 3A, Gong et al., 1996). A similar pattern was observed for the depth-averaged DIP in the upper 10 m. DIP concentrations of $>0.1 \mu\text{mol P L}^{-1}$ only occurred near the coastal region north to latitude 28°N (Fig. 3E). Excess nitrate was only observed in the coastal zone near the Changjiang mouth, indicating that nitrogen was enriched in the terrestrial discharge (Fig. 3I). During this cruise, in situ APA values ranged $6\text{--}75 \text{ pmol PO}_4^{3-} (\mu\text{g Chl. } a)^{-1} \text{ min}^{-1}$ in the ECS. Low activities were observed in the coastal zone with a pattern that coincided well with the DIP-rich zone. However, low APA

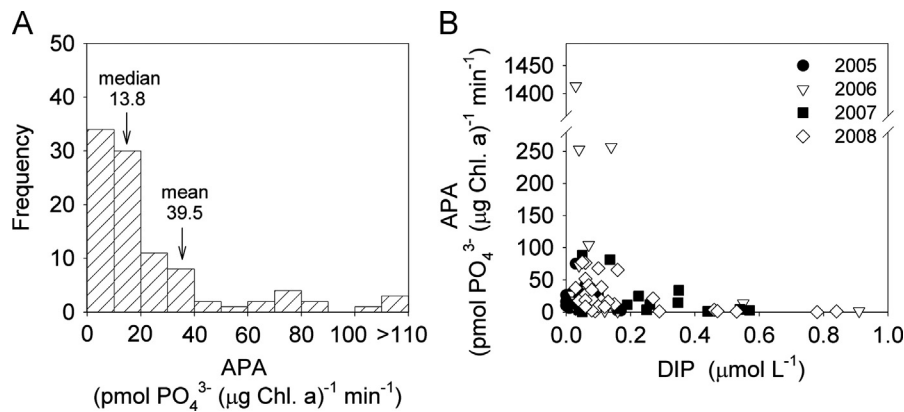


Fig. 2. Descriptive statistics of alkaline phosphatase activity (APA) measured in the East China Sea during 2005–2008. (A) The frequency distribution of the APA for all data points. The 3 APA values higher than 120 were 253, 257, and 1414 $\text{pmol PO}_4^{3-} (\mu\text{g Chl. a})^{-1} \text{min}^{-1}$, respectively. (B) Relationship between APA and the concentration of dissolved inorganic phosphate (DIP).

values also appeared at some locations where ambient DIP was $< 0.1 \mu\text{mol P L}^{-1}$ (Fig. 2B), such as Sts. 1 and 24 (Fig. 3M). In the coastal region, the microphytoplankton was mainly composed of diatoms and dinoflagellates (Table 2). In contrast, high APA values were observed in the central mid-shelf area with the highest value reaching $75.1 \text{ pmol PO}_4^{3-} (\mu\text{g Chl. a})^{-1} \text{min}^{-1}$ at St. 31a (Fig. 3M), and the microphytoplankton community was dominated by dinoflagellates (Table 2). The high values of APA were responsive to ambient phosphate concentration. For example, APA at St. 31a substantially decreased to $39.2 \text{ pmol PO}_4^{3-} (\mu\text{g Chl. a})^{-1} \text{min}^{-1}$ by the addition of extra orthophosphate (Table 2).

3.3. Distributions of Changjiang plume, DIP, N_{ex} and APA in 2006

Compared to observations in June 2005, the plume size in June–July 2006 was significantly larger, and covered almost the entire northwestern area of the ECS (Fig. 3B). The distribution of DIP was spatially correlated with that of salinity, with concentrations of $> 0.1 \mu\text{mol P L}^{-1}$ observed in both the Changjiang plume and an elongated area along the coast (Fig. 3F). Excess nitrate was still observed near the Changjiang mouth with a tendency to extend southward along the coast until latitude 28°N (Fig. 3J). High APA values only occurred in the northeastern corner of the ECS, and the highest value of $1414 \text{ pmol PO}_4^{3-} (\mu\text{g Chl. a})^{-1} \text{min}^{-1}$ occurred at St. 23. From this high APA center, moderately high values expanded southeasterly, and the region sandwiched between the 2 APA contour lines of $10 \text{ pmol PO}_4^{3-} (\mu\text{g Chl. a})^{-1} \text{min}^{-1}$ formed a J-shaped area fringing the region with excess nitrate (Fig. 3N). Dinoflagellates were the dominant microphytoplankton in this J-shaped area, and the addition of extra phosphate effectively suppressed APA (Table 2).

3.4. Distributions of Changjiang plume, DIP, N_{ex} , APA, and F_v/F_m in 2007

During the cruise in July 2007, the Changjiang plume was again in a reduced phase, and was restricted to a small region near the river mouth (Fig. 3C). The plume still contained a high concentration of DIP, but a second high-DIP region appeared in the coastal zone near 28°N latitude. This second high-DIP region extended eastward to the mid-shelf zone with concentrations of $> 0.1 \mu\text{mol P L}^{-1}$ (Fig. 3G). Excess nitrate was only observed in the coastal zone near the Changjiang mouth (Fig. 3K). The vertical profiles of temperature near 28°N latitude revealed that the thermoclines became shallower toward the coast (Fig. 4A and B), which suggested that the second high-DIP region came from a coastal upwelling. Surface excess nitrate of St. 30 was low at

$4 \mu\text{mol N L}^{-1}$, indicating that the chemical characteristics of seawater near 28°N latitude differed from those of the Changjiang plume (Fig. 4D and E). During this cruise, APA values ranged 0.32 – $88.5 \text{ pmol PO}_4^{3-} (\mu\text{g Chl. a})^{-1} \text{min}^{-1}$ in the ECS. High values were observed in 2 regions (Fig. 3O). One was in the northeast area of the ECS with the highest value of $88.5 \text{ pmol PO}_4^{3-} (\mu\text{g Chl. a})^{-1} \text{min}^{-1}$ at St. 28, and APA values decreasing radially from this center. The other high APA region was in the southwestern quadrant of the ECS, and the highest value was $81.4 \text{ pmol PO}_4^{3-} (\mu\text{g Chl. a})^{-1} \text{min}^{-1}$ at St. 3. The phosphate addition caused APA at St. 28 to fall from 88.5 to $26.4 \text{ pmol PO}_4^{3-} (\mu\text{g Chl. a})^{-1} \text{min}^{-1}$ (Table 2), and similar results were obtained at other stations (Fig. 5). Values of the maximum quantum efficiency of photosynthesis (F_v/F_m) varied 0.22 – 0.51 in the ECS (Fig. 3Q). High F_v/F_m values were mainly observed in the coastal zone and formed a triangular region extending seaward from St. 30, which then gradually decreased toward the shelf break. Diatoms were the dominant microphytoplankton, and were rich in *Chaetoceros* spp. and *Guinardia* spp. In comparison, dinoflagellates were much less abundant (Table 2).

3.5. Distributions of Changjiang plume, DIP, N_{ex} , APA, and F_v/F_m in 2008

In July 2008, the size of the Changjiang plume had moderately increased compared to that in 2007 (Fig. 3D). The high-DIP region with concentrations exceeding $0.1 \mu\text{mol P L}^{-1}$ occurred in an elongated area adjacent to the coast (Fig. 3H). Excess nitrate was observed near the Changjiang mouth with a distribution pattern similar to those in previous cruises (Fig. 3L). Since the DIP-rich region extended beyond the southern limit of the excess nitrate region, and since the thermoclines became shallower toward the shore, a coastal upwelling was apparently the source of this additional nutrient in this region (Fig. 4C and F). APA values ranged 0.19 – $77.7 \text{ pmol PO}_4^{3-} (\mu\text{g Chl. a})^{-1} \text{min}^{-1}$ (Fig. 3P). Low values mainly occurred in the coastal zone, but a string of low-APA stations was also observed between Sts. 6 and 1A. *Chaetoceros* spp., *Rhizosolenia* spp., and *Cylindrotheca closterium* were the dominant diatoms with certain amount of coexistent dinoflagellates (Table 2). The rest of the continental shelf was occupied by stations with high activities, and APA values exceeding $60 \text{ pmol PO}_4^{3-} (\mu\text{g Chl. a})^{-1} \text{min}^{-1}$ were observed at St. 31 in the mid-shelf region and Sts. 10 and 24 near the shelf break (Fig. 3P). Both diatoms and dinoflagellates were present at these stations, and the phosphate addition was still effective in suppressing APA (Table 2 and Fig. 5). Values of F_v/F_m in July 2008 varied 0.25 – 0.57 . F_v/F_m values of > 0.4 were observed in the coastal zone, but high

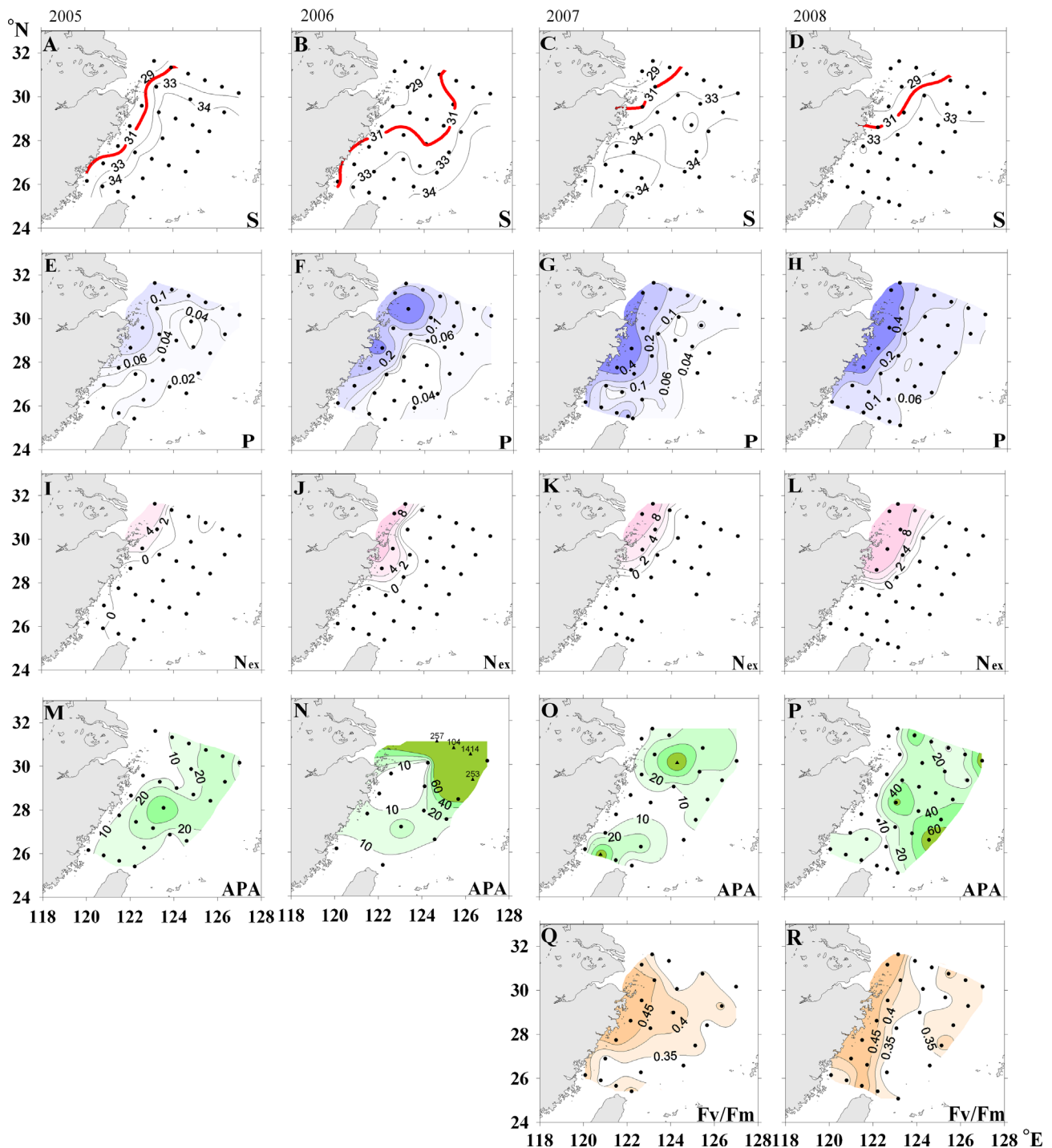


Fig. 3. Spatial distributions of hydrographic and biological parameters in the East China Sea. (A–D) Salinity (psu), (E–H) dissolved inorganic phosphate concentration (μM), (I–L) excess nitrogen based on nitrite and nitrate measurements (μM), (M–P) chlorophyll (Chl)-*a*-specific alkaline phosphatase activity (APA, $\text{pmol PO}_4^{3-} (\mu\text{g Chl. } a)^{-1} \text{min}^{-1}$), and (Q, R) maximum quantum efficiency of photosynthesis (F_v/F_m). The red line in panels A–D is the 31 isohaline traditionally used to mark the edge of the Changjiang river plume. Solid triangles in panels N and P are APAs $> 80 \text{ pmol PO}_4^{3-} (\mu\text{g Chl. } a)^{-1} \text{min}^{-1}$.

values were also observed at 2 offshore stations which formed an extension of the coastal high value patch (Fig. 3R).

3.6. The relationship between APA and F_v/F_m

An overall comparison of APA and F_v/F_m obtained in 2007 and 2008 revealed certain degree of correlation between these 2 parameters. When F_v/F_m was in the high range of 0.5–0.6, APA was always low (Fig. 6A). In contrast, when F_v/F_m was in the low range of 0.2–0.3, APA varied substantially, which revealed that high APA

and low F_v/F_m coexisted in only a subset of all stations. The method of quantile regression thus was used to differentiate 2 types of APA- F_v/F_m relationship. Data pairs above the quantile-regression line of median APA were strong-response stations at which APA sensitively increased with decreasing F_v/F_m , and a statistically significant regression coefficient of -187.4 ($p < 0.01$, $r^2 = 0.35$) was obtained (Fig. 6B). In contrast, data pairs below the quantile-regression line were weak-response stations with a regression coefficient of -55.7 ($p < 0.001$, $r^2 = 0.52$) which indicated a more gentle slope of the regression line (Fig. 6B).

Table 2

Chlorophyll (Chl.) *a* concentrations ($\mu\text{g L}^{-1}$) and species compositions of net-collected microphytoplankton at selected stations with typical low and high values of alkaline phosphatase activity (APA) in the East China Sea. Chl. *a* was measured in both natural seawater (in situ) and net-collected samples (net-tow). APAs were measured in net-collected samples (in situ APA) and in samples with added phosphate (P-suppressed APA, $\text{pmol PO}_4^{3-} (\mu\text{g Chl. } a)^{-1} \text{min}^{-1}$). F_p/F_m , maximum quantum efficiency of photosynthesis. Diatom and dinoflagellate abundances are reported as cells mL^{-1} , and *Trichodesmium* abundance is reported as trichomes mL^{-1} . –, no sample taken.

	Low-APA stations				High-APA stations			
	2005 St. 4	2006 St. 4	2007 St. 4	2008 St. 4	2005 St. 31a	2006 St. 22	2007 St. 28	2008 St. 20
Chl. <i>a</i> (in situ)	1.34	1.51	0.95	0.43	0.18	1.57	0.34	0.59
Chl. <i>a</i> (net-tow)	188	312	72.0	36.7	3.08	13.5	13.6	11.8
In situ APA	6.24	5.39	4.96	18.0	75.1	104	88.5	65.5
P-suppressed APA	6.35	5.76	1.65	7.76	39.2	50.7	26.4	12.3
F_p/F_m	–	–	0.45	0.37	–	–	0.34	0.27
Diatoms								
<i>Chaetoceros</i> spp.	250	62,250	5563	17,188	0	0	8000	79
<i>Cylindrotheca closterium</i>	0	1500	125	1094	0	0	0	1827
<i>Rhizosolenia</i> spp.	2000	750	188	3594	0	0	0	9
<i>Hemiaulus</i> spp.	250	500	188	156	0	0	0	0
<i>Guinardia</i> spp.	7875	250	1875	156	0	0	0	0
<i>Skeletonema</i> spp.	0	5500	125	6875	0	0	0	9
<i>Pseudonitzschia</i> spp.	0	4625	125	2031	0	0	1438	0
<i>Leptocylindrus</i> spp.	32,500	3250	0	7813	0	0	0	0
<i>Asterionellopsis</i> spp.	0	0	2438	0	0	0	0	0
Other species	6125	11,925	8937	1250	38	0	10,437	61
Dinoflagellates								
<i>Ceratium</i> spp.	750	125	0	0	25	25	0	115
<i>Dinophysis</i> spp.	0	0	0	0	13	13	0	0
<i>Prorocentrum</i> spp.	0	0	0	0	0	0	0	20
<i>Protoperidinium</i> spp.	125	1000	0	156	25	0	0	173
Other species	750	0	250	0	163	262	0	0
Cyanobacteria								
<i>Trichodesmium</i> spp.	0	0	625	0	100	0	0	9

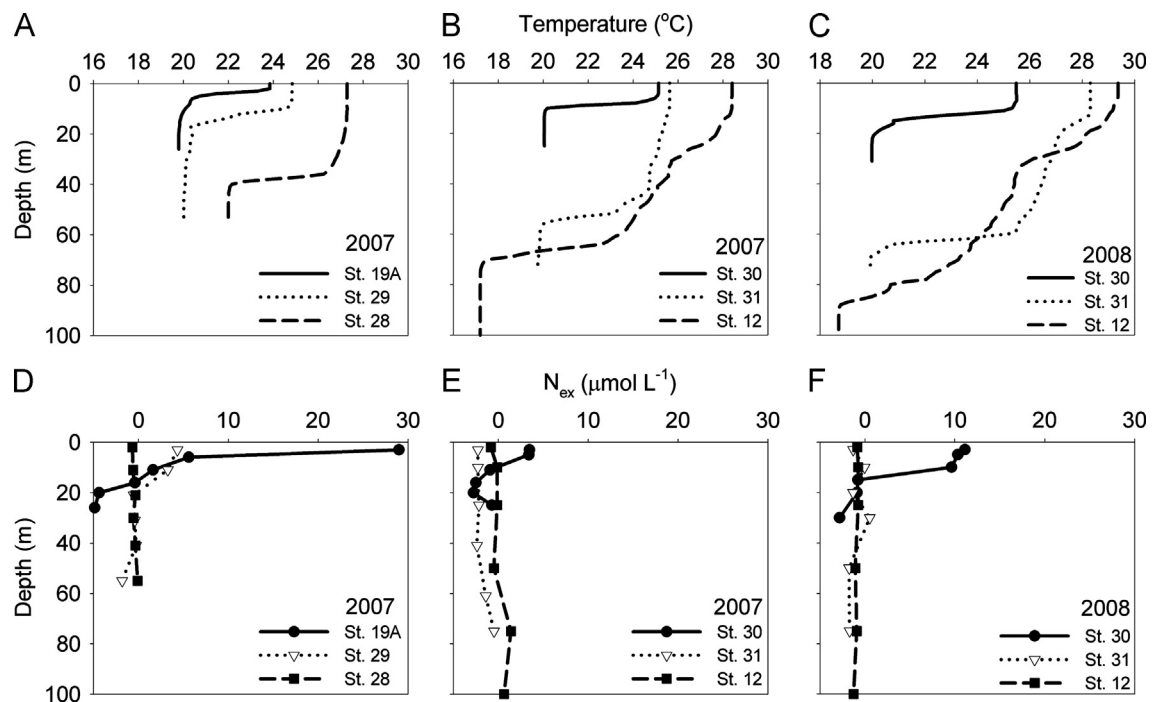


Fig. 4. Vertical profiles of temperature and nitrate in excess showing cross-shelf variations. (A) Temperature profiles along a northern transect passing through the Changjiang river plume in 2007. (B) Temperature profiles along a mid-ECS transect starting from a coastal high-DIP region near 28°N in 2007. (C) Temperature profiles along a mid-ECS transect in 2008. (D–F) Profiles of excess nitrate along the above mentioned 3 transects.

4. Discussion

In our results, high values of APA rarely occurred when DIP exceeded $0.2 \mu\text{mol P L}^{-1}$ (Fig. 2B), indicating that high concentration of ambient DIP leads to the status of phosphorus sufficiency in

microphytoplankton. However, both high and low APA values were observed when DIP concentration was low. In this category, the phosphate addition experiment demonstrated that all APAs higher than $30 \text{ pmol PO}_4^{3-} (\mu\text{g Chl. } a)^{-1} \text{min}^{-1}$ were effectively suppressed by $69.4 \pm 4.9\%$ (95% confidence limits) (Fig. 5B), implying

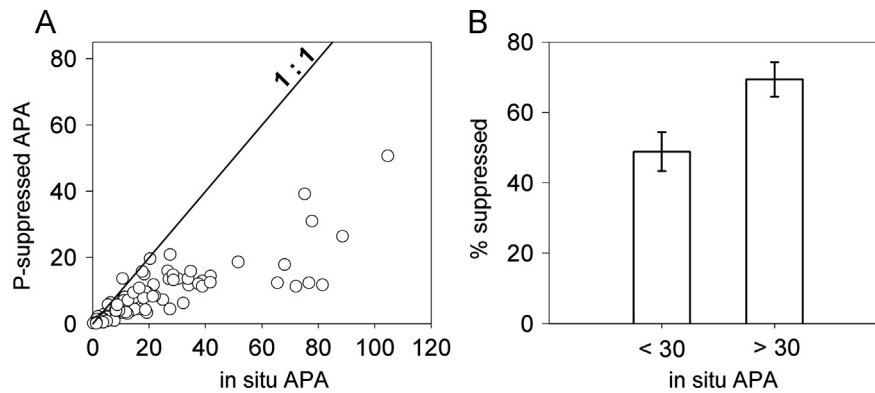


Fig. 5. Decreases in microplankton alkaline phosphatase activities due to the addition of extra phosphate in summer cruises to the East China Sea between 2005 and 2008. (A) Relationship between in situ and P-suppressed APAs. The diagonal line marks the 1:1 relationship between the 2 variables, and 3 outliers with an in situ APA > 120 pmol PO₄³⁻ (μg Chl. a)⁻¹ min⁻¹ were not shown. (B) Differential suppressions observed between the subgroup with in situ APAs < 30 pmol PO₄³⁻ (μg Chl. a)⁻¹ min⁻¹ and the subgroup with in situ APAs > 30 pmol PO₄³⁻ (μg Chl. a)⁻¹ min⁻¹. Error bars marked the 95% confidence limits of subgroup means.

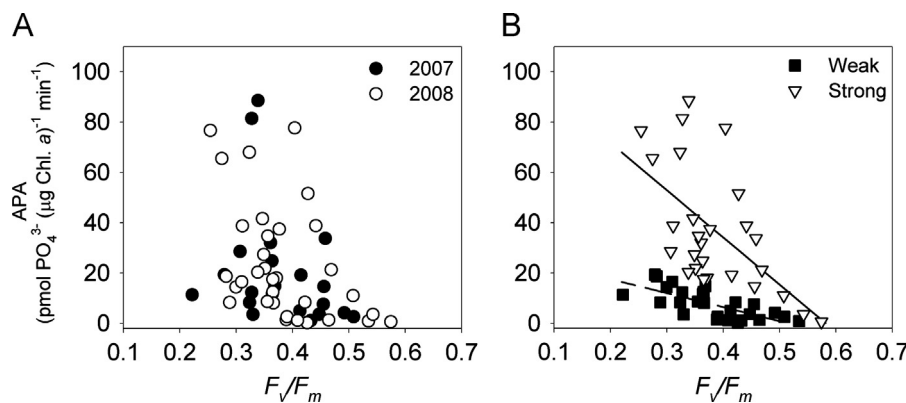


Fig. 6. Relationship between alkaline phosphatase activity (APA) and the maximum quantum efficiency of photosynthesis (F_v/F_m) during 2 summer cruises to the East China Sea. (A) Relationships observed in 2007 (filled circles) and 2008 (open circles). (B) The differentiation between the weak- (filled squares) and the strong-response (open triangles) stations in the East China Sea based on the 0.5 quantile-regression line. The solid line is the linear relationship of strong-response stations ($y = -187.4x + 109.2$, $p < 0.01$, $r^2 = 0.35$) and the dashed line is the relationship of weak-response stations ($y = -55.7x + 28.7$, $p < 0.001$, $r^2 = 0.52$) in the ECS.

that high values of APA were caused by P deficiency. As for stations with a low APA and a low concentration of DIP, plausible explanations included a limiting nutrient other than phosphorus, dominate species using deep phosphate via vertical migration, and dominant species with genetically inherited low APA (Olsson and Granéli, 1991; Dyhrman and Ruttenberg, 2006; Nicholson et al., 2006).

In our results, we did not observe a significant correlation between APA and phytoplankton species composition. Stations with high APA values were not necessarily dominated by dinoflagellates ($p > 0.05$, Supplementary Fig. S1). At certain stations (e.g., St. 28 in 2007, Table 2), microphytoplankton were dominated by diatoms, but the associated APA values were still high. In Sargasso Sea, Lomas et al. (2004) observed that a higher percentage of diatoms expressed this enzyme in comparison to dinoflagellates. Similarly, measured F_v/F_m values in the ECS were unrelated to either the presence of filamentous cyanobacteria or that of dinoflagellates ($p > 0.05$, Supplementary Fig. S1), suggesting weak influences from species composition (Lomas et al., 2004; Yamaguchi et al., 2005; Nicholson et al., 2006).

If we assume that F_v/F_m is a general indicator of nutrient-controlled quantum efficiency and APA is a specific indicator of phosphorus stress, stations in the ECS can be categorized as either strong-responsive or weak-responsive to F_v/F_m (Fig. 6B). At strong-response stations, low F_v/F_m values were consistently accompanied by high APAs. This negative correlation between APA and F_v/F_m matched the September trend observed in 2007 when

phosphorus stress was induced by a strong front blocking the mixing between an upwelling system and Kuroshio Current (Liu et al., 2010). In contrast, low F_v/F_m values were accompanied by a very limited increase in APA at weak-response stations (Fig. 6B), suggesting that low quantum efficiency was not related to phosphorus stress at these stations.

An examination of the geographical distribution of strong-response stations revealed their close association with Changjiang river plume (Fig. 7). In addition to low salinities, Changjiang river plume is also characterized by the presence of excess nitrate (Wong et al., 1998). Although the calculation of N_{ex} does not include ammonium (Eq. (1)), its influence on the distribution of N_{ex} ratio in the ECS should be small. According to a survey conducted in 2007, the ammonium concentrations were high in the plum region, reaching 3.5 μM at St. 19A (Gong, unpublished result). Ammonium concentration rapidly decreased beyond the plume, and became < 0.3 μM near the shelf break. As a result, the inclusion of ammonium in N_{ex} makes the Changjiang river plume a more nitrogen-enriched environment, but has a limited impact on the rest of the ECS.

In both 2007 and 2008, regions composed of strong-response stations assumed a cross-shelf distribution pattern extended eastward from the coastal zone near Changjiang river mouth. Some strong-response stations also occurred near the entrance of Taiwan Strait in the southern ECS, but the area occupied by these stations was much smaller (Fig. 7). Within the strong-response region in the northern ECS, stations with low APA, high F_v/F_m , and high nutrients

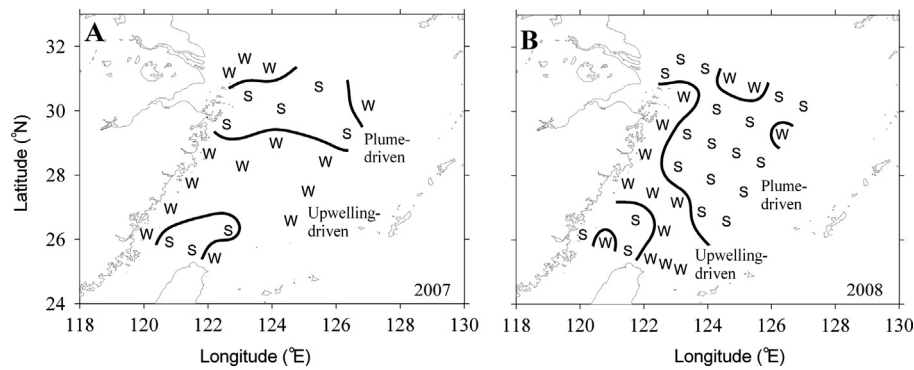


Fig. 7. Geographical distributions of the weak-response (W) and the strong-response (S) stations in the East China Sea based on the relationship between alkaline phosphatase activity (APA) and F_v/F_m . (A) Distribution in 2007, (B) distribution in 2008. The Changjiang discharge and upwelled waters were used to explain the formation of the weak- and strong-response stations.

were observed in the Changjiang river plume (Fig. 3). Although the Changjiang discharge has an N:P ratio much higher than the Redfield ratio (Fig. 3K and L), microphytoplankton at these stations did not show symptoms of nutrient stress. This is in agreement with the statement that phytoplankton do not experience nitrogen or phosphorus stress if nutrient concentrations exceed $2 \mu\text{mol N L}^{-1}$ or $0.1 \mu\text{mol P L}^{-1}$, respectively (Dortch and Whitledge, 1992). As the water drifted away from the river mouth, mixing and phytoplankton uptake reduced its phosphorus content, and the situation of high APA and low F_v/F_m began to develop beyond the edge of the river plume (Fig. 3O–R). Similar spatial patterns of P stress were observed in other marine systems, including the southern ECS and northern Red Sea (Li et al., 1998; Liu et al., 2010). The transition from nutrient-rich stations to phosphorus-stressed stations in the northern ECS can be viewed as a plume-driven mixing series.

In contrast, the weak-response stations occupied a section of ECS to the south of the strong-response region (Fig. 7). Within the weak-response region, most nutrient-rich stations were in the coastal zone, but excess nitrate was not observed in their surface layer (Fig. 3). Coastal upwelling in the ECS driven by the summer monsoon and prevailing currents was confirmed in a recent report (Chen et al., 2004), and profiles of hydrographic parameters at coastal stations in summer 2007 and 2008 supported the presence of upwellings (Fig. 4). Although high in nutrients, upwelled waters are relatively rich in phosphorus compared to the Changjiang discharge (Chen et al., 2004). The cross-shelf mixing between upwelled water and offshore waters generated the transition of F_v/F_m from high to low values, but the increase in APA was very limited (Figs. 3 and 6B). The axis of this upwelling-driven mixing series can be visually traced by an offshore-extending string of stations with $F_v/F_m > 0.4$ and $\text{APA} < 10 \text{ pmol PO}_4^{3-} (\mu\text{g Chl. } a)^{-1} \text{ min}^{-1}$ (Fig. 3Q,R). Microphytoplankton at the offshore end of this mixing series suffered low photosynthetic efficiency, but this situation was not caused by a shortage of phosphorus.

The plume-driven and the upwelling-driven mixing series showed substantial interannual variations in their distributions and relative strengths (Fig. 3). Coastal upwelling was inconspicuous in 2005 and 2006, so microphytoplankton experiencing P stress created a complete J-shaped region of high APA fringing the Changjiang plume. When the Changjiang plume expanded in 2006, the increased nutrient supply prolonged the uptake of phosphorus, and the J-shaped region was pushed further offshore (Fig. 3J). In 2007 and 2008, the Changjiang plume retreated to a small area near the river mouth, and coastal upwelling was strong (Fig. 3C and D). As a result, a high-APA region occurred at locations very close to the river mouth, and was limited to the northern ECS as the upwelling-driven mixing series on the south prevented the development of P stress in microphytoplankton (Fig. 3K and L).

Net-collected samples contain concentrated phytoplankton cells in an environment very different from their natural habitat. To avoid potential modifications in APA and F_v/F_m values, samples in this study were carefully collected and measurements were completed in 1–2 h after collection. Similar procedures have been used for physiological measurements in other studies on microphytoplankton (Berman-Frank et al., 2001; Villareal, 1992), and Perry (1972) mentioned that phytoplankton may need more than 24 h to generate additional AP. On the other hand, a low concentration of AP substrate at $0.11 \mu\text{mol L}^{-1}$ was used according to the original protocol (Perry, 1972). A short incubation time of 30 min was employed to avoid extensive reduction in substrate concentration. Based on a comparative experiment conducted in the ECS, APAs measured at substrate concentrations of 0.11 and $2.2 \mu\text{mol P L}^{-1}$, respectively, are well correlated ($r=0.91$, Liu, 2010). Admittedly, an extensive reduction in substrate concentration during incubation may occur at a small number of stations. Considering the amount of substrate consumed, however, these stations would still possess high but somewhat underestimated values of APA, which should not affect the general distribution of phosphorus-stressed regions.

In conclusion, our results indicated that the Changjiang plume and coastal upwelling are 2 important hydrographic features that influence the phosphorus status of microphytoplankton during summer in the ECS. Although the plume water contained nitrogen in excess of phosphorus, both APA and F_v/F_m values indicated that microphytoplankton in the nutrient-rich river plume did not experience P stress. Instead, a region with high APA usually formed beyond the edge of the river plume, and its size changed considerably with the expansion and retreat of the plume. To the south of the river plume, coastal upwelling frequently occurred, and provided nutrients with a more-balanced N:P ratio. When the upwelled water gradually mixed with offshore waters, the quantum efficiency decreased without the symptom of P stress. According to our study, microphytoplankton in the northern ECS are constantly experiencing P stress beyond the outer limit of the Changjiang plume in summer. In contrast, the status of phosphorus stress in the southern ECS is more variable, depending on the strength of coastal upwelling and the formation of fronts (Liu et al., 2010).

Acknowledgments

We thank the captains and the crew of the *R/V Ocean Researcher I and II* for their assistance during the cruises. We are also grateful to H.-F. Wang for measuring trichome lengths, and to S.-H. Hung for his assistance with F_v/F_m measurements. This study was

supported in part by research grants from the R.O.C. National Science Council (NSC101-2611-M-019-016 and NSC101-2313-B-019-006) and in part by funds from the Center of Excellence for the Oceans, National Taiwan Ocean University.

Appendix A. Supporting information

Supplementary data associated with this article can be found in the online version at <http://dx.doi.org/10.1016/j.csr.2013.04.017>.

References

- Berglund, J., Müren, U., Båmstedt, U., Andersson, A., 2007. Efficiency of a phytoplankton-based and a bacteria-based food web in a pelagic marine system. *Limnology Oceanography* 52, 121–131.
- Berman-Frank, I., Lundgren, P., Chen, Y.B., Küpper, H., Kolber, Z., Bergman, B., Falkowski, P., 2001. Segregation of nitrogen fixation and oxygenic photosynthesis in the marine cyanobacterium *Trichodesmium*. *Science* 294, 1534–1537.
- Campbell, D., Hurry, V., Clarke, A.K., Gustafsson, P., Oquist, G., 1998. Chlorophyll fluorescence analysis of cyanobacterial photosynthesis and acclimation. *Microbiology and Molecular Biology Reviews* 62, 667–683.
- Canfield, D.E., Glazer, A.N., Falkowski, P.G., 2010. The evolution and future of earth's nitrogen cycle. *Science* 330, 192–196.
- Chang, J., 2000. Precision of different methods used for estimating the abundance of nitrogen-fixing marine cyanobacterium, *Trichodesmium* Ehrenberg. *Journal of Experimental Marine Biology and Ecology* 245, 215–224.
- Chang, J., Shiah, F.K., Gong, G.C., Chiang, K.P., 2003. Cross-shelf variation in carbon-to-chlorophyll *a* ratios in the East China Sea summer 1998. *Deep-Sea Research II* 50, 1237–1248.
- Chen, Y.L.L., 2000. Comparisons of primary productivity and phytoplankton size structure in the marginal regions of southern East China Sea. *Continental Shelf Research* 20, 437–458.
- Chen, Y.L.L., Chen, H.Y., Gong, G.C., Lin, Y.H., Jan, S., Takahashi, M., 2004. Phytoplankton production during a summer coastal upwelling in the East China Sea. *Continental Shelf Research* 24, 1321–1338.
- Cullen, J.J., Davis, R.F., 2003. The blank can make a big difference in oceanographic measurements. *The Limnology and Oceanography Bulletin* 12, 30–35.
- Dortch, Q., Whitledge, T.E., 1992. Does nitrogen or silicon limit phytoplankton production in the Mississippi River plume and nearby regions? *Continental Shelf Research* 12, 1293–1309.
- Dyrman, S.T., Ruttenberg, K.C., 2006. Presence and regulation of alkaline phosphatase activity in eukaryotic phytoplankton from the coastal ocean: implications for dissolved organic phosphorus remineralization. *Limnology Oceanography* 51, 1381–1390.
- Falkowski, P.G., 2002. The ocean's invisible forest. *Scientific American* 287, 56–61.
- Geider, R.J., Laroche, J., Greene, R.M., Olaizola, M., 1993. Response of the photosynthetic apparatus of *Phaeodactylum tricorutum* (Bacillariophyceae) to nitrate, phosphate, or iron starvation. *Journal of Phycology* 29, 755–766.
- Glibert, P.M., 2010. Long-term changes in nutrient loading and stoichiometry and their relationships with changes in the food web and dominant pelagic fish species in the San Francisco estuary. *California Reviews in Fish Science* 18, 211–232.
- Gong, G.C., 1992. Chemical hydrography of the kuroshio front in the sea northeast of Taiwan. National Taiwan University, Taipei, Taiwan. (Ph.D. thesis).
- Gong, G.C., Chen, Y.L.L., Liu, K.K., 1996. Chemical hydrography and chlorophyll *a* distribution in the East China Sea in summer: implications in nutrient dynamics. *Continental Shelf Research* 16, 1561–1590.
- Gong, G.C., Shiah, F.K., Liu, K.K., Wen, Y.H., Liang, M.H., 2000. Spatial and temporal variation of chlorophyll *a* primary productivity and chemical hydrography in the southern East China Sea. *Continental Shelf Research* 20, 411–436.
- Harrison, P.J., Hu, M.H., Yang, Y.P., Lu, X., 1990. Phosphate limitation in estuarine and coastal waters of China. *Journal of Experimental Marine Biology and Ecology* 140, 79–87.
- Huang, B., Ou, L., Wang, X., Huo, W., Li, R., Hong, H., Zhu, M., Qi, Y., 2007. Alkaline phosphatase activity of phytoplankton in the East China Sea coastal water with frequent harmful algal bloom occurrences. *Aquatic Microbial Ecology: International Journal* 49, 195–206.
- Karl, D.M., Tien, G., 1997. Temporal variability in dissolved phosphorus concentrations in the subtropical North Pacific Ocean. *Marine Chemistry* 56, 77–96.
- Kjørboe, T., 1993. Turbulence, phytoplankton cell size, and the structure of food webs. *Advances in Marine Biology* 29, 1–72.
- Koenker, R., Hallock, K.F., 2001. Quantile Regression. *Journal of Economic Perspectives: A Journal of the American Economic Association* 15, 143–156.
- Kolber, Z., Falkowski, P.G., 1993. Use of active fluorescence to estimate phytoplankton photosynthesis in situ. *Limnology Oceanography* 38, 1646–1665.
- Kromkamp, J., Peene, J., 1999. Estimation of phytoplankton photosynthesis and nutrient limitation in the Eastern Scheldt estuary using variable fluorescence. *Aquatic Ecology* 33, 101–104.
- Li, Hong., Veldhuis, M.J.W., Post, A.F., 1998. Alkaline phosphatase activities among planktonic communities in the northern Red Sea. *Marine Ecology Progress Series* 173, 107–115.
- Liu, H.C., 2010. Applications and Improvements of Alkaline Phosphatase Activity Assay as a Phosphorus-Deficiency Indicator in Microphytoplankton. National Taiwan Ocean University, Keelung, Taiwan. (Ph.D. thesis).
- Liu, H.C., Gong, G.C., Chang, J., 2010. Lateral water exchange between shelf-margin upwelling and Kuroshio waters influences phosphorus stress in microphytoplankton. *Marine Ecology Progress Series* 409, 121–130.
- Lomas, M.W., Swain, A., Shhilton, R., Ammerman, J.W., 2004. Taxonomic variability of phosphorus stress in Sargasso Sea phytoplankton. *Limnology Oceanography* 46, 2303–2310.
- Nicholson, D., Dyrman, S., Chavez, F., Paytan, A., 2006. Alkaline phosphatase activity in the phytoplankton communities of Monterey Bay and San Francisco Bay. *Limnology Oceanography* 51, 874–883.
- Olsson, P., Granéli, E., 1991. Observation on diurnal vertical migration and phased cell division for three coexisting marine dinoflagellates. *Journal of Plankton Research* 13, 1313–1324.
- Ou, L., Huang, B., Lin, L., Hong, H., Zhang, F., Chen, Z., 2006. Phosphorus stress of phytoplankton in the Taiwan Strait determined by bulk and single-cell alkaline phosphatase activity assays. *Marine Ecology Progress Series* 327, 95–106.
- Pai, S.C., Yang, C.C., Riley, J.P., 1990a. Effects of acidity and molybdate concentration on the kinetics of the formation of the phosphoantimonymolybdenum blue complex. *Analytica Chimica Acta* 299, 115–120.
- Pai, S.C., Yang, C.C., Riley, J.P., 1990. Formation kinetics of the pink azo dye in the determination of nitrite in natural waters. *Analytica Chimica Acta* 299, 345–349.
- Perry, M.J., 1972. Alkaline phosphatase activity in subtropical Central North Pacific waters using a sensitive fluorometric method. *Marine Biology* 15, 113–119.
- Seitzinger, S.P., Kroeze, C., Bouwman, A.F., Caraco, N., Dentener, F., Styles, R.V., 2002. Global patterns of dissolved inorganic and particulate nitrogen inputs to coastal systems: recent conditions and future projections. *Estuaries* 25, 640–655.
- Smayda, T.J., 1974. Some experiments on the sinking characteristics of two freshwater diatoms. *Limnology Oceanography* 19, 628–635.
- Sommer, U., Stibor, H., Katchakis, A., Sommer, F., Hansen, T., 2002. Pelagic food web configurations at different levels of nutrient richness and their implications for the ratio fish production: primary production. *Hydrobiologia* 84, 11–20.
- Tomas, C.R., Hasle, G.R., Syvertsen, E.E., Steidinger, K.A., Tangen, K., 1996. Identifying Marine Diatom and Dinoflagellates. Academic Press, San Diego.
- Villareal, T.A., 1992. Buoyancy properties of the giant diatom *Ethmodiscus*. *Journal of Plankton Research* 14, 459–463.
- Wang, S.L., Chen, C.T.A., Hong, G.H., Chung, C.S., 2000. Carbon dioxide and related parameters in the East China Sea. *Continental Shelf Research* 20, 525–544.
- Welschmeyer, N.A., 1994. Fluorometric analysis of chlorophyll *a* in the presence of chlorophyll *b* and pheopigments. *Limnology Oceanography* 39, 1985–1992.
- Wong, G.T.F., Gong, G.C., Liu, K.K., Pai, S.C., 1998. 'Excess nitrate' in the East China Sea. *Estuarine, Coastal and Shelf Science* 46, 411–418.
- Wykoff, D.D., Davies, J.P., Melis, A., Grossman, A.R., 1998. The regulation of photosynthetic electron transport during nutrient deprivation in *Chlamydomonas reinhardtii*. *Plant Physiology* 117, 129–139.
- Yamaguchi, H., Sakou, H., Fukami, K., Adachi, M., Yamaguchi, M., Nishijima, T., 2005. Utilization of organic phosphorus and production of alkaline phosphatase by the marine phytoplankton, *Heterocapsa circularisquama*, *Fibrocapsa japonica* and *Chaetoceros ceratosporum*. *Plankton Biology and Ecology* 52, 67–75.